Optical Design of InAlGaAs Low-Loss Tunnel-Junction Apertures for Long-Wavelength Vertical-Cavity Lasers

D. Feezell, D. A. Buell, D. Lofgreen, M. Mehta, and L. A. Coldren, *Fellow, IEEE*

***Abstract*—We report on the optical design of thin selectively etched InAlGaAs tunnel-junction apertures for the realization of optically efficient long-wavelength vertical-cavity surface-emitting lasers (VCSELs). These apertures were designed to introduce minimal optical loss to the structure, facilitate single-mode operation, and yield optical mode diameters that better match the injected current density profile. We then demonstrate InP-based VCSELs emitting at 1304 nm utilizing these low-loss InAlGaAs apertures, resulting in optically efficient low-loss devices with differential quantum efficiencies of up to 60%.**

***Index Terms*—Aperture, InAlGaAs, InP-based, long wavelength, semiconductor laser processing, semiconductor lasers, tunnel junction, vertical-cavity surface-emitting lasers (VCSELs).**

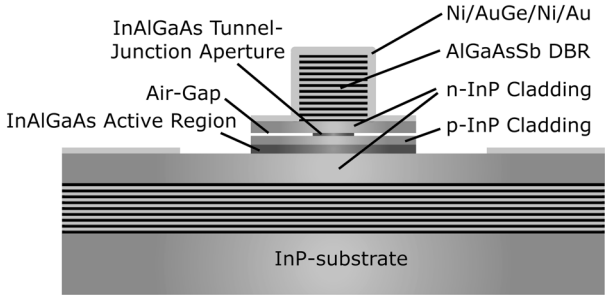

Fig. 1. Schematic of bottom-emitting all-epitaxial VCSEL structure with undercut thin tunnel-junction aperture.

I. Introduction

LONG-wavelength vertical-cavity surface-emitting lasers (VCSELs) emitting in the 1300–1600-nm wavelength range are attractive light sources for short to midrange optical fiber communications. These devices target low-loss and low-dispersion windows in standard optical fibers and are expected to provide a low-cost alternative to the existing edge-emitting infrastructure. With low power consumption, on-wafer testing, simple packaging, and high fiber-coupling efficiency, VCSELs are ideal transmitters for metro, local area, and storage area networks.

Recently, many promising long-wavelength VCSEL results have been demonstrated [1]–[5]. However, it is still desirable to continually demonstrate devices with significantly reduced optical loss. More optically efficient structures with low internal loss will facilitate reduced threshold currents and enable higher differential quantum efficiencies. These are desirable characteristics for achieving improved modulation performance with lower required drive currents.

Previously, our group has reported InP-based devices operating in the 1300–1600-nm wavelength region [6], [7]. These devices utilized well-established InAlGaAs active region technology and AlGaAsSb distributed Bragg reflectors (DBRs). This combination facilitates monolithic all-epitaxial InP-based devices spanning the entire long-wavelength telecommunications band. With this platform, we have recently demonstrated devices with efficient modulation characteristics and high differential quantum efficiencies [8]. The high differential quantum efficiencies observed resulted from the implementation of thin selectively etched tunnel-junction apertures for low-loss optical guiding [9]. In this work, we describe the optical design of these thin selectively etched tunnel-junction apertures. First, the free carrier absorption (FCA) loss from the highly doped tunnel-junction layer is minimized. Then, using a two-dimensional model of the optical cavity, thin selectively etched tunnel-junction apertures are designed to provide effective guiding of the fundamental lateral mode with low scattering loss. We then fabricate and characterize optically efficient single-mode 1304-nm InP-based VCSELs utilizing these apertures, with devices demonstrating high differential quantum efficiencies of greater than 60%, optical efficiencies up to 80%, and single-mode continuous-wave operation up to 90 °C.

The bottom-emitting device structure is shown in Fig. 1 for reference and is the same as previously reported [7]. A $1/2-\lambda$ InAlGaAs multiple-quantum-well active region is clad on both sides by InP layers. Intracavity contacts are made to these InP layers, allowing for the AlGaAsSb DBRs to remain undoped. Embedded within the upper InP cladding layer is a 35-nm n^{++}-InAlGaAs–p^{++}-InAlGaAs tunnel-junction layer that is selectively etched to form a thin air-gap aperture for electrical and optical confinement. Details regarding the fabrication of these devices have been previously reported [7]–[9].

Manuscript received February 14, 2006; revised March 2, 2006. This work was supported in part by the National Science Foundation.

D. Feezell and L. A. Coldren are with the Department of Electrical and Computer Engineering and the Department of Materials, University of California, Santa Barbara, CA 93106 USA (e-mail: feezell@engineering.ucsb.edu).

D. A. Buell is with CNRS-CRHEA, 06560 Valbonne, France.

D. Lofgreen is with Raytheon Vision Systems, Goleta, CA 93117 USA.

M. Mehta is with the University of New Mexico, Albuquerque, NM 87131 USA.

Digital Object Identifier 10.1109/JQE.2006.874007

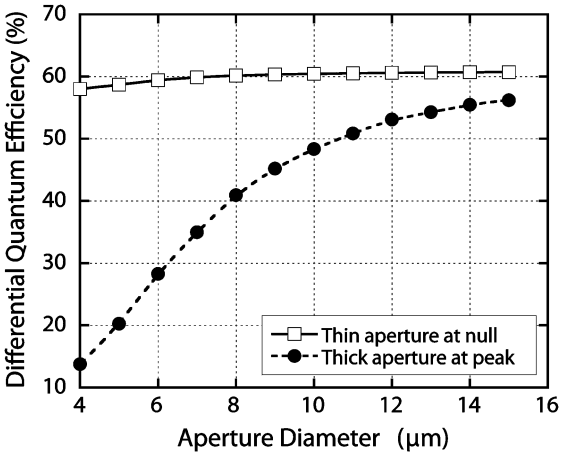

Fig. 2. Simulated differential efficiencies for an active region apertured device and a tunnel-junction apertured device, demonstrating the scaling benefits provided by thin apertures.

II. Motivation for Thin Tunnel-Junction Apertures

Despite the promising results previously obtained by our group, these devices employed a rather inefficient aperturing scheme [6], [10]. A thick (200 nm) undercut active region aperture, inherently placed at standing wave peak, was employed for optical confinement. The strong guiding effect of this thick aperture introduced a significant amount of scattering loss to the devices. In fact, up to 60% of the total internal loss in these devices was due to aperture scattering of the mode. As a result, these devices only achieved differential quantum efficiencies of 23%. Additionally, these devices suffered from increased sidewall recombination at the thick exposed etched active region [10]. The implementation of thin tunnel-junction apertures alleviates these problems by providing low-loss optical confinement, avoiding exposed active region sidewalls, and generating an injected current density profile that better matches the shape of the optical mode.

An additional benefit provided by thin low-loss apertures is the ability to scale the aperture diameters to smaller dimensions without introducing increased scattering loss. As an example, Fig. 2 shows a simulation of predicted differential efficiencies for the previously reported devices with a thick active region aperture and the thin tunnel-junction apertured devices of this work. These differential efficiencies are estimated from the calculated loss in the devices (i.e., aperture scattering loss and FCA loss). The loss calculation will be explained in subsequent sections. Fig. 2 is intended to demonstrate the trend between scaling to smaller dimensions for both aperturing schemes. It is clear that the thin tunnel-junction aperturing scheme maintains a more constant differential quantum efficiency value down to smaller aperture dimensions. This is an important benefit for realizing higher differential quantum efficiency devices with lower threshold currents.

III. Tunnel-Junction Aperture Optical Design

With the goal of limiting optical loss in the structure, reduction of the FCA loss introduced by the tunnel junction layer is of prime importance. The placement of the tunnel junction relative to the optical standing wave in the cavity and its thickness are critical design issues due to the high doping (N_A = 1e20 cm^{-3}, N_D = 3e19 cm^{-3}) required in the tunnel junction layer to achieve efficient quantum tunneling. The tunnel junction aperture layer should be designed to minimize the single-pass optical loss. For a tunnel junction with a thickness $L = L_n + L_p$, where L_n and L_p are the thicknesses of the n and p sides of the junction, respectively, the single-pass optical loss is calculated by $1 - e^{-\alpha_i L \Gamma_{\rm enh}}$. Here, α_i is the internal optical loss from FCA and $\Gamma_{\rm enh}$ is the standing-wave enhancement factor [11]. In order to minimize the single-pass optical loss from a highly doped layer, such as the tunnel junction, $\Gamma_{\rm enh}$ and L must be minimized. The standing wave enhancement factor can be minimized to some extent by selectively placing the highly doped tunnel-junction layer at an optical standing wave null in the cavity, as shown in Fig. 3. This reduces the overlap between the highly doped tunnel-junction layer and regions of high electric field. To illustrate the importance of the standing-wave enhancement factor on optical loss, the FCA loss introduced by the tunnel junction as a function of its relative position to the optical standing-wave null was calculated and is shown in Fig. 4. For variations from the null in the range of tens of nanometers, we observe an order of magnitude increase in FCA loss.

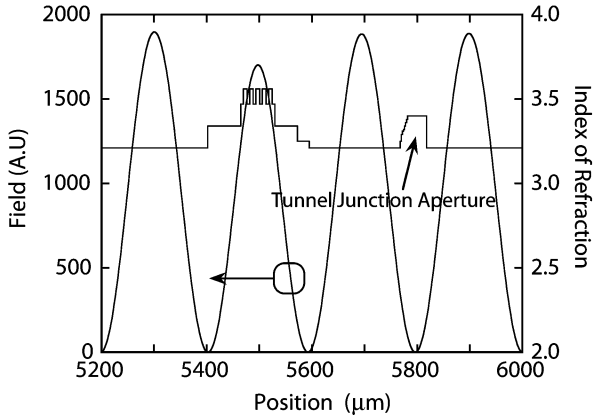

Fig. 3. Electric field and index profile in the cavity of the structure, showing the placement of the tunnel junction aperture layer at an optical standing wave null for the minimization of the standing-wave enhancement factor.

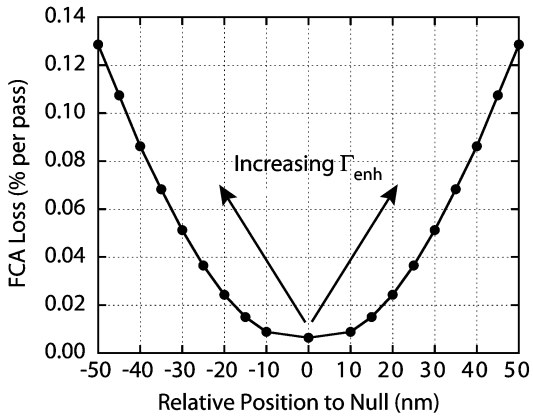

Fig. 4. Simulated FCA loss from the tunnel-junction layer as a function of variation from its placement at an optical standing-wave null.

Another method to further limit the FCA loss from the tunnel-junction layer is to reduce its thickness. This also relaxes epi-

taxial growth tolerances. However, due to restrictions on doping levels and quantum tunneling probability, there are practical minimum allowable values for the junction thicknesses, L_n and L_p. These values can be calculated via the WKB method reported by Mars, *et al.* [12]. For the InAlGaAs tunnel junctions in this work, these values were determined to be in the range of 10–20 nm. Specifically, for the reported devices, $L_n = 20$ nm and $L_p = 15$ nm.

The figure of merit employed for the optical design of the etched aperture is the effective index perturbation to the optical mode, $\Delta n_{\text{eff}} = n_{\text{eff}}^{\text{core}} - n_{\text{eff}}^{\text{undercut}}$, where $n_{\text{eff}}^{\text{core}}$ and $n_{\text{eff}}^{\text{undercut}}$ are the effective indexes in the growth direction of the core and undercut regions of the aperture, respectively. This treatment yields a two-dimensional index profile that provides a simple optical model of the aperture. For a given physical aperture diameter, the index perturbation determines the important optical properties of the aperture, specifically the effective optical mode diameter and the aperture scattering loss. Constraints on these parameters predominately determine the allowed index perturbation introduced by the aperture. If the index perturbation is too small, the optical mode diameter may be significantly larger than the injected current density profile, leading to increased absorption loss in the unpumped areas of the quantum wells. Conversely, if the index perturbation is too large, the optical mode may experience significantly increased scattering loss. Therefore, as described below, an index perturbation is chosen that provides effective guiding with minimal scattering loss.

To determine the waveguide eigenmodes, and thus the effective optical mode diameter, the two-dimensional scalar wave equation was solved on this index profile using a finite difference technique with a nonuniform mesh [13]–[15]. The calculated effective optical mode diameters (determined at the $1/e^2$ point of the normalized mode amplitude) for the fundamental lateral mode versus the physical aperture diameter, are shown in Fig. 5(a) for various values of Δn_{eff}. For high differential quantum efficiencies and reduced threshold currents, increased overlap between the optical mode and the current density profile is desired. Since current spreading is minimal in the p-InP beneath the tunnel junction aperture, the current density profile is primarily determined by the physical aperture diameter. Therefore, for optimal modal gain, the effective optical mode diameter should be similar to the physical aperture diameter. Effective optical mode diameters larger than the physical aperture diameter will lead to increased absorption loss from overlap of the optical mode tails with unpumped regions of the quantum wells. For mechanically stable single-mode devices, aperture diameters in the range of 6–8 μm are desired. From Fig. 5(a), it is determined that a Δn_{eff} in the range of 0.005 to 0.01 is required to satisfy the above guiding condition.

The optical scattering loss associated with the aperture was then examined by propagating the optical mode through an unfolded cavity. The procedure implemented is similar to that described by Fox and Li [13]–[15]. As the field is propagated, a position-dependent phase shift, a position-dependent gain, and an absorption are applied to the mode. The phase shift, described by $\phi(x, y) = k_0 \Delta n_{\text{eff}}(x, y) L_{\text{cav}}$, where k_0 is the free space wave vector and L_{cav} is the effective cavity length, is what approximates the effect of the aperture in the model. The phase,

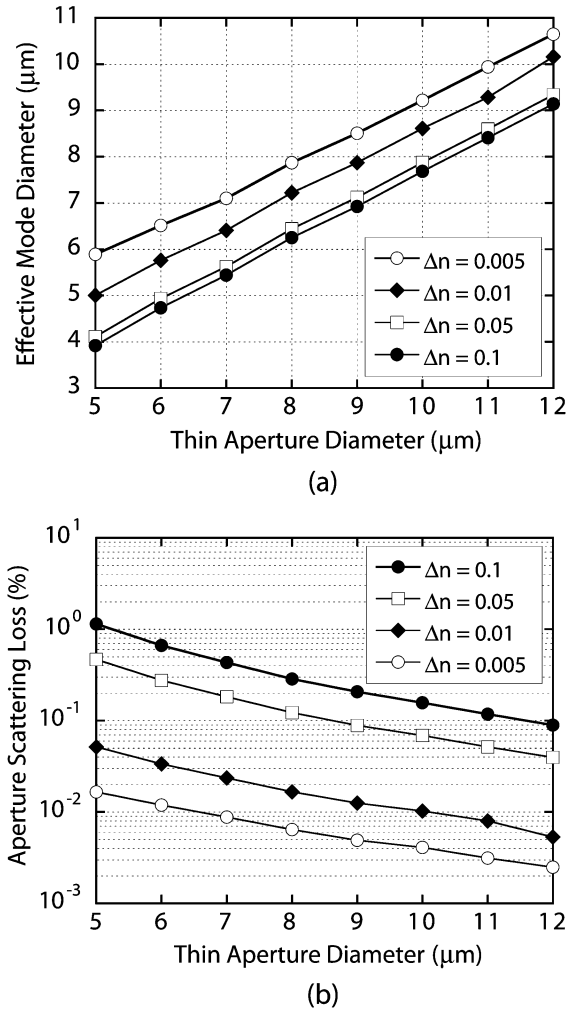

Fig. 5. (a) Calculated effective optical mode diameter for the fundamental mode versus physical aperture diameter for various aperture strengths. (b) Calculated aperture scattering loss versus physical aperture diameter for various aperture strengths.

gain, and absorption values are continually adjusted until there is only a phase shift associated with a pass through the cavity. At this point, the mode of the system and the gain are known. The scattering loss is then determined from the modal gain. Fig. 5(b) shows the calculated aperture scattering loss versus physical aperture diameter for various values of Δn_{eff}. From the figure, the values of Δn_{eff} needed to achieve the required effective optical mode diameters determined above (i.e., —$\Delta n_{\text{eff}} \approx 0.005$ to 0.01) produce apertures that contribute very little scattering loss to the structure. This result is in stark contrast to our previously reported thick etched active region apertures placed at an optical standing wave peak ($\Delta n_{\text{eff}} = 0.10$) and represents over an order of magnitude reduction in optical loss [10].

Although it is possible to further limit optical scattering loss from the aperture by reducing Δn_{eff} below 0.005, quantum tunneling probability requires a tunnel-junction thickness on the order of 35 nm, which already introduces a Δn_{eff} of nearly 0.005. Additionally, the restrictions stated above regarding the effective optical mode diameter do not allow for such low values of Δn_{eff}, and by the analysis above, it was determined that a selectively etched aperture with $\Delta n_{\text{eff}} = 0.01$ effectively guides

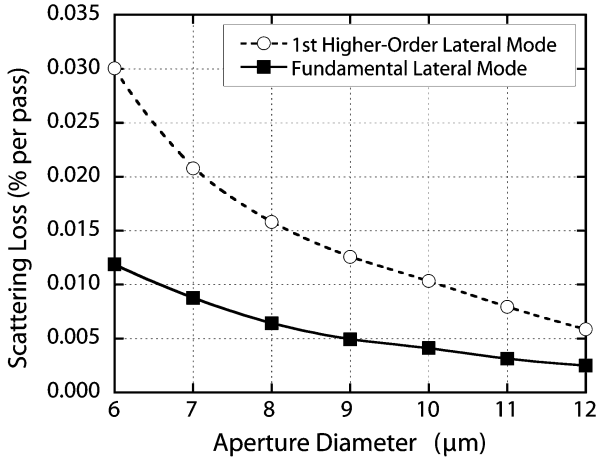

Fig. 6. Calculated aperture scattering loss ($\Delta n_{\text{eff}} = 0.005$) per pass for the fundamental lateral mode and the next higher order lateral mode as a function of aperture diameter, demonstrating the increased scattering loss experienced by higher order modes.

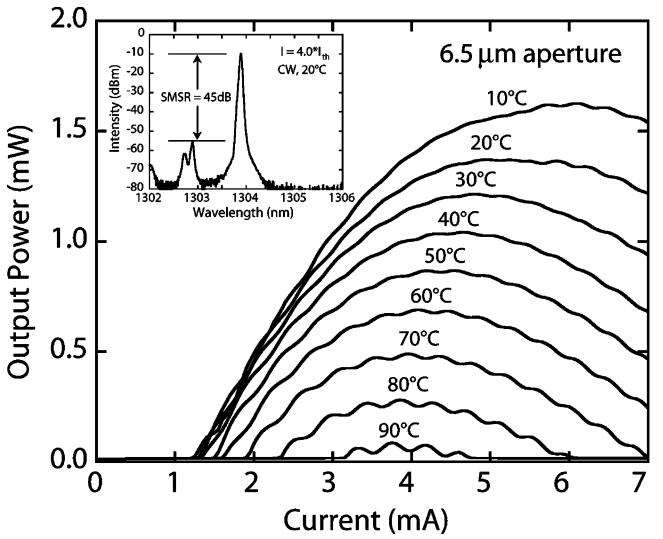

Fig. 7. Continuous-wave light versus current curves for various stage temperatures, showing high room-temperature differential quantum efficiency of 60%. The inset shows the lasing spectrum, demonstrating single-mode behavior with a 45-dB SMSR.

the optical mode while still introducing very little scattering loss. $\Delta n_{\text{eff}} = 0.005$ was not chosen in order to avoid operating near the limit of the optical mode becoming larger than the current density profile. Since the 35-nm n^{++}-InAlGaAs–p^{++}-InAlGaAs tunnel junction did not quite achieve the necessary $\Delta n_{\text{eff}} = 0.01$, a section of etchable lowly doped and compositionally graded InAlGaAs was placed adjacent to the tunnel junction layer to increase Δn_{eff} to the desired value of 0.01. This grade is shown near the tunnel junction aperture in Fig. 3.

Finally, to achieve single-mode operation, an effective aperture design should suppress higher order lateral modes from lasing. As discussed above, the effective optical mode diameter of the fundamental mode was designed to closely mimic the current density profile, ensuring this mode reaches lasing at the lowest possible threshold. Moreover, due to the shapes of the higher order modes, they typically experience increased scattering loss from the aperture, thus further increasing their lasing thresholds. A comparison between the calculated scattering loss experienced by the fundamental lateral mode and the first higher order lateral mode for an aperture with $\Delta n_{\text{eff}} = 0.005$ is shown in Fig. 6. For aperture diameters in the range of 6–8 μm, we observe an increase in scattering loss of several times for the next higher order mode. This additional loss further ensures single-mode lasing operation of the fundamental mode at these aperture dimensions.

IV. Results and Discussion

A VCSEL structure with the designed low-loss tunnel-junction aperture ($\Delta n_{\text{eff}} = 0.01$) was then grown by molecular beam epitaxy in a single growth step [16]. Devices were then fabricated and characterized. Fig. 7 shows the continuous-wave light versus current characteristics for a device with a 6.5-μm aperture diameter. This device achieved a high continuous-wave differential quantum efficiency of 60% at room-temperature and operated up to 90 °C, the highest reported temperature operation for a VCSEL with Sb-based DBRs. The lasing spectrum is also inset in Fig. 7 and demonstrates strong single-mode behavior with a side-mode suppression ratio (SMSR) of 45 dB. These results, particularly the high differential quantum efficiency, clearly indicate the effectiveness of the optical design of the low-loss aperture and represent a significant improvement over the previously reported work. As a result of the differential quantum efficiency values observed, the optical efficiency of these devices was also quite high. The optical efficiency η_0 is calculated by $\eta_0 = \eta_d/\eta_i$, where η_d is the differential quantum efficiency and η_i is the injection efficiency as determined from edge-emitting lasers with the same active region structure [11]. Conceptually, η_0 is the percentage of photons generated in the active region that leave the optical cavity through the desired DBR mirror and are collected as useful output. Since the injection efficiency was determined to be 75% by the method referenced above, the optical efficiency is therefore calculated to be 80%.

As evidenced by the high differential quantum efficiencies these devices achieved, the internal optical loss was very low. This was largely a result of the design and implementation of the thin tunnel-junction aperture. However, several other factors contributed to the performance. The DBRs were undoped to limit optical loss and very smooth, with the entire epitaxial structure displaying an RMS roughness of only 3.1 Å. Furthermore, the implementation of tunnel junctions limited the incorporation of highly absorbing p-type material.

The known contributions to optical loss in the devices from FCA and aperture scattering were estimated. The FCA loss for each section of the device was determined by overlapping the optical mode with the doping profile in the structure and the aperture scattering loss was calculated by the method described above. The results of these calculations are shown in Table I. The total calculated internal loss in the structure due to FCA and aperture scattering is shown to be $\approx$0.16% per pass ($\approx$5 cm^{-1}). We believe this to be a significantly low number for a long-wavelength VCSEL. Although the FCA loss reported here and the FCA loss reported in our previous devices is similar, the

TABLE I
CALCULATED LOSS CONTRIBUTIONS FROM VARIOUS SOURCES IN THE DEVICE

Loss Source	Loss (% per pass)
Aperture Scattering	0.0287
Tunnel Junction (FCA)	0.0234
p-InP Cladding (FCA)	0.0743
n-InP Cladding (FCA)	0.0350
Active Region (FCA)	0.0005
Total Calculated Internal Loss	**0.1619**

aperture scattering loss has been reduced by approximately one order of magnitude in this work.

The internal loss can also be experimentally obtained to verify our calculated estimations. By the method described by Coldren and Corzine, the measured VCSEL differential quantum efficiency, the calculated VCSEL mirror loss, and the injection efficiency obtained from InAlGaAs edge-emitting lasers are utilized to obtain the internal loss [11]. This method yields an experimental internal loss value of $\approx 6\ \mathrm{cm}^{-1}$, just slightly higher than the calculated estimate. The small discrepancy in the experimentally obtained value from the calculated value is explained by the presence of unaccounted for loss, such as macroscopic defect sites and surface roughness.

V. SUMMARY AND CONCLUSIONS

In conclusion, we have designed thin selectively etched tunnel-junction apertures for more efficient optical confinement in InP-based long-wavelength VCSELs. These apertures were designed to provide effective guiding of the optical mode, while introducing minimal optical loss to the structure. We have then grown, fabricated, and characterized VCSELs utilizing these low-loss air-gap apertures. The resulting optically efficient devices yielded low internal loss estimates, demonstrated differential quantum efficiencies of 60%, and achieved single-mode operation up to 90 °C.

REFERENCES

[1] N. Nishiyama, C. Caneau, S. Tsuda, G. Guryanov, M. Hu, R. Bhat, and C. Zah, "10-Gb/s error-free transmission under optical reflection using isolator-free 1.3-μm InP-based vertical-cavity surface-emitting lasers," *IEEE Photon. Technol. Lett.*, vol. 17, no. 8, pp. 1605–1607, Aug. 2005.

[2] J. Chang, C. L. Shieh, X. Huang, G. Liu, M. V. R. Murty, C. C. Lin, and D. X. Xu, "Efficient CW lasing and high-speed modulation of 1.3 μm AlGaInAs VCSELs with good high temperature lasing performance," *IEEE Photon. Technol. Lett.*, vol. 17, no. 1, pp. 7–9, Jan. 2005.

[3] M. Ortsiefer, K. Windhorn, G. Bohm, J. Rosskopf, R. Shau, E. Ronneberg, W. Hofman, and M. Amann, "2.5-mW single-mode operation of 1.55-μm buried tunnel junction VCSELs," *IEEE Photon. Technol. Lett.*, vol. 17, no. 8, pp. 1596–1598, Aug. 2005.

[4] V. Iakovlev, G. Suruceneau, A. Caliman, A. Mereuta, C. Berseth, A. Syrbu, A. Rudra, and E. Kapon, "High-performance single-mode VCSELs in the 1310-nm waveband," *IEEE Photon. Technol. Lett.*, vol. 17, no. 5, pp. 947–949, Jan. 2005.

[5] V. Jayaraman, M. Mehta, A. W. Jackson, S. Wu, Y. Okuno, J. Piprek, and J. E. Bowers, "High-Power 1320-nm wafer-bonded VCSELs with tunnel junctions," *IEEE Photon. Technol. Lett.*, vol. 15, no. 11, pp. 1495–1497, Nov. 2004.

[6] S. Nakagawa, E. Hall, G. Almuneau, J. K. Kim, D. A. Buell, H. Kroemer, and L. A. Coldren, "88 °C, continuous-wave operation of apertured, intracavity contacted, 1.55 μm vertical-cavity surface-emitting lasers," *Appl. Phys. Lett.*, vol. 78, pp. 1337–1339, 2001.

[7] D. Feezell, D. A. Buell, and L. A. Coldren, "Continuous wave operation of all-epitaxial InP-based 1.3 μm VCSELs with 57% differential quantum efficiency," *Electron. Lett.*, vol. 41, no. 14, pp. 803–804, Jul. 2005.

[8] D. Feezell, L. A. Johansson, D. A. Buell, and L. A. Coldren, "Efficient modulation of InP-based 1.3 μm VCSELs with AsSb-based DBRs," *IEEE Photon. Technol. Lett.*, vol. 17, no. 11, pp. 2253–2255, Nov. 2005.

[9] D. Feezell, D. A. Buell, and L. A. Coldren, "InP-based 1.3–1.6 μm VCSELs with selectively etched tunnel-junction apertures on a wavelength flexible platform," *IEEE Photon. Technol. Lett.*, vol. 17, no. 10, pp. 2017–2019, Oct. 2005.

[10] S. Nakagawa, "InP-Lattice-Matched, Long-Wavelength Vertical-Cavity Surface-Emitting Lasers for Optical Fiber Communications," Ph.D. dissertation, Dept. Elect. and Comp. Eng., University of California Santa Barbara, Santa Barbara, CA, 2001.

[11] L. A. Coldren and S. W. Corzine, *Diode Lasers and Photonic Integrated Circuits*. New York: Wiley, 1995.

[12] D. E. Mars, Y. L. Chang, M. H. Leary, S. D. Roh, and D. R. Chamberlin, "Low-resistance tunnel junctions on GaAs substrates using GaInNAs," *Appl. Phys. Lett.*, vol. 84, pp. 2560–2562, 2004.

[13] A. G. Fox and T. Li, "Resonant modes in a maser interferometer," *Bell Syst. Tech. J.*, vol. 40, pp. 453–488, 1961.

[14] E. R. Hegblom, D. I. Babic, B. J. Thibeault, and L. A. Coldren, "Scattering losses from dielectric apertures in vertical-cavity lasers," *IEEE J. Sel. Top. Quantum Electron.*, vol. 3, no. 2, pp. 379–386, Apr. 1997.

[15] D. Lofgreen, "Investigation of selective quantum well intermixing in vertical cavity lasers," Ph.D. dissertation, Dept. Elect. Comp. Eng., Univ. California, Santa Barbara, 2004.

[16] D. A. Buell, D. Feezell, and L. A. Coldren, "Molecular beam epitaxy of AlGaAsSb-based long-wavelength vertical-cavity lasers," *J. Vac. Sci. Technol. B*, to be published.

Daniel F. Feezell received the B.S. degree in electrical engineering from the University of California, Irvine, in 2000. He then joined Prof. L. Coldren's group at the University of California, Santa Barbara, where he received the M.S. and Ph.D. degrees in 2001 and 2005, respectively.

He is currently working on design, fabrication, and characterization of novel GaN-based light-emitting devices as a Postdoctoral Researcher under Prof. S. Nakamura at the University of California, Santa Barbara.

David A. Buell received the Ph.D. degree in materials from the University of California, Santa Barbara (UCSB), in 2005 for his work on InP-based vertical cavity lasers.

He is a Researcher in molecular beam epitaxy of III–V and II–IV semiconductors with a focus on optoelectronics and optical phenomena, UCSB. He is currently researching ZnO at CNRS-CRHEA, Valbonne, France, as a Chateaubriand Fellow.

Dan Lofgreen received the B.S. degrees in both electrical and computer engineering from Iowa State University, Ames, in 1997. He then joined Prof. L. Coldren's group at the University of California, Santa Barbara, where he received the M.S. and Ph.D. degrees in 1999 and 2004, respectively.

He is currently working on design, growth, and characterization of HgCdTe-based infrared detectors at Raytheon Vision Systems, Goleta, CA.

Manish Mehta received the Ph.D. degree in electrical engineering from the University of California, Santa Barbara, in February 2006.

He is currently working on the development of midinfrared semiconductor lasers as a Postdoctoral Researcher under Dr. D. Huffaker at the University of New Mexico, Albuquerque.

Larry A. Coldren (S'67–M'72–SM'77–F'82) received the Ph.D. degree in electrical engineering from Stanford University, Stanford, CA, in 1972.

After 13 years in the research area at Bell Laboratories, he was appointed Professor of Electrical and Computer Engineering at the University of California at Santa Barbara (UCSB) campus in 1984. In 1986, he assumed a joint appointment with Materials and ECE, and in 2000 the Fred Kavli Chair in Optoelectronics and Sensors. He is also Chairman and Chief Technology Officer of Agility Communications, Inc. At UCSB, his efforts have included work on novel guided-wave and vertical-cavity modulators and lasers as well as the underlying materials growth and fabrication technology. He is now investigating the integration of various optoelectronic devices, including optical amplifiers and modulators, tunable lasers, wavelength-converters, and surface-emitting lasers. He has authored or coauthored over 500 papers, five book chapters, one textbook, and has been issued 32 patents.

Prof. Coldren is a Fellow of the Optical Society of America (OSA) and a past Vice-President of IEEE Laser and Electro-Optics Society (LEOS), the recipient of the 2004 John Tyndall Award, and a member of the National Academy of Engineering.